

# Supercritical Water Confined In Graphene Nanochannels

J. Sala\*, E. Guàrdia, and J. Martí

Departament de Física i Enginyeria Nuclear, Universitat Politècnica de Catalunya, B4-B5  
Campus Nord, 08034 Barcelona, Catalonia, Spain

e-mail:jonas.sala@upc.edu & FAX:+34934017100

We report results of a series of molecular dynamics simulations of water inside a narrow graphite channel at supercritical conditions. A wide range of densities ( $0.08\text{-}0.66\text{ gcm}^{-3}$ ) at the supercritical temperature of 673 K have been considered. A thorough analysis of the structure, hydrogen bonding, dielectric and dynamic properties of the systems was performed. Our present results are compared with previous studies of liquid water confined in graphene nanochannels at ambient and high temperature conditions.

## INTRODUCTION

Recent advances in the design of nuclear reactors are related to the so called Supercritical Water Reactor, where confined supercritical water is employed as the coolant medium [1]. Our contribution will present brand new computer simulations of supercritical water confined in graphene slabs as an extension of previous works [2,3,4]. Structure and hydrogen bonding, as well as dielectric and dynamical properties of supercritical water confined in those graphene slabs have been investigated by molecular dynamics (MD) simulations. In this paper we will be focused on the structure, hydrogen bonding and dielectric properties. Dynamic properties will be published elsewhere [5].

## I - COMPUTATIONAL DETAILS

We considered  $N$  water molecules embedded into two parallel graphite plates with no defects to model two sheets of highly oriented pyrolytic graphite (HOPG). We set up a simulation box in the  $x$ ,  $y$ , and  $z$  directions of 34.4, 34.1 and 31 Å, respectively. These values correspond to the geometry of HOPG in the real system. We assumed the  $z$  coordinate to be perpendicular to the graphite layers, and the usual periodic boundary conditions were considered only in the  $x$  and  $y$  directions. The temperature of the system was kept at  $T=673\text{K}$ . Different number of molecules were assumed ranging from  $N=100$  to  $N=800$  to cover a range of densities from  $\rho=0.08$  to  $\rho=0.66\text{ gcm}^{-3}$ . Snapshots of typical MD configurations are depicted in Figure 1.

Water-water inter- and intramolecular interactions were modeled with a flexible simple-point-charge (SPC) potential which was specifically reparametrized to reproduce the main trends of the infrared spectrum of water at ambient conditions [6]. This flexible SPC potential has a critical point ( $T_c = 643\text{ K}$ ,  $\rho_c = 0.32\text{ gcm}^{-3}$ ) which is very close to the experimental one ( $T_c = 647\text{ K}$ ,  $\rho_c = 0.322\text{ gcm}^{-3}$ ) [7]. Water-carbon forces were assumed to be of the Lennard-Jones type with the same parametrization employed in previous studies of water near graphite (see for instance Ref. [8]).

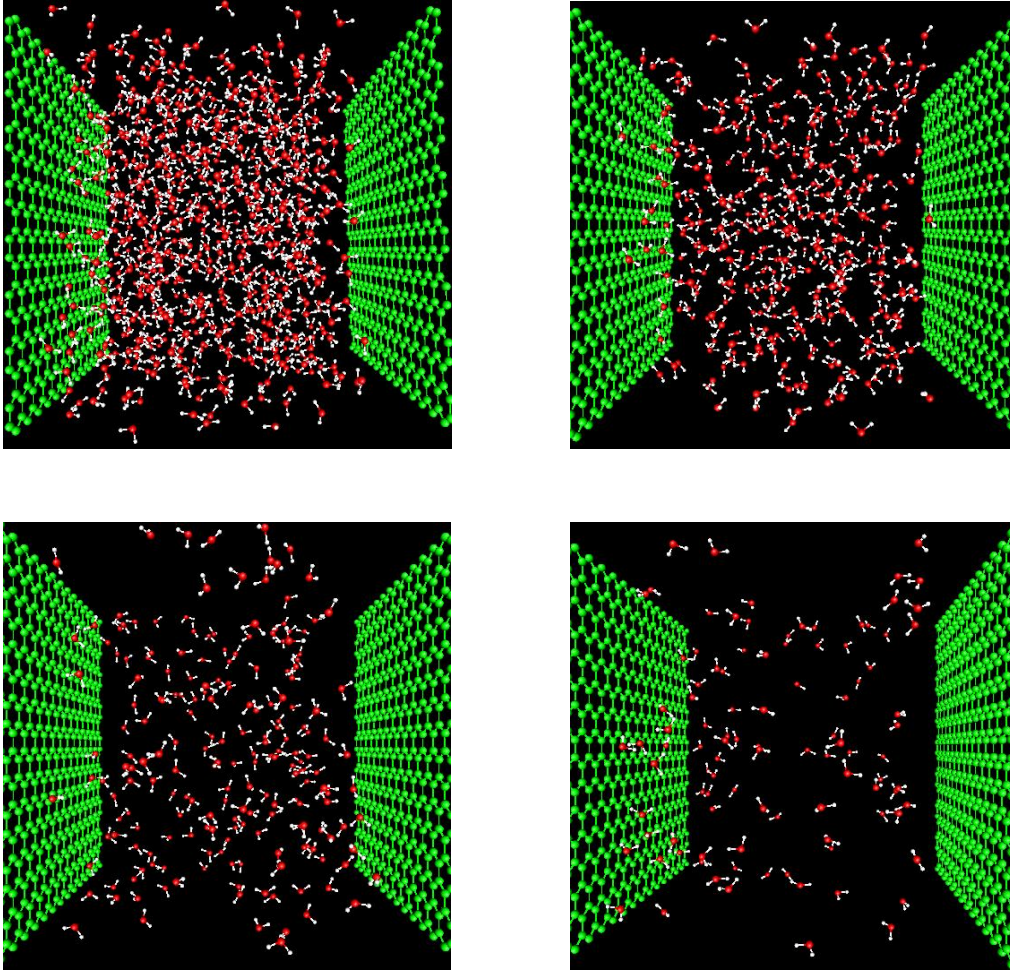


**Figure 1:** Snapshots of the simulation box with the water molecules and the graphene walls at different densities (from left to right and from top to bottom  $\rho=0.66, 0.33, 0.16$  and  $0.08 \text{ g/cm}^3$ ).

To carry out the simulations we employed the integration algorithm of Berendsen et al. [9] with a time step of 0.5 fs and a thermal bath coupling parameter of 10 fs. Short-ranged forces were truncated at half the box length and the Ewald summation technique as proposed by Spohr [10] was applied to account for the long ranged Coulomb interaction. Each run consisted of an initial equilibration period of 50 ps and a production period of 300 ps to collect statistically meaningful properties.

## II – RESULTS AND DISCUSSION

During the simulations, we separately analyzed the properties of two different groups of water molecules directly related to their locations with respect to the graphite walls: adsorbed for water in the closest layer and bulk for water far from the graphite. The exact definition of these regions in each case comes from the corresponding oxygen density profiles. (see Figure 2). As can be seen from Figure 2, the peaks related to the interfacial structure become less well defined as the density of the system diminishes.

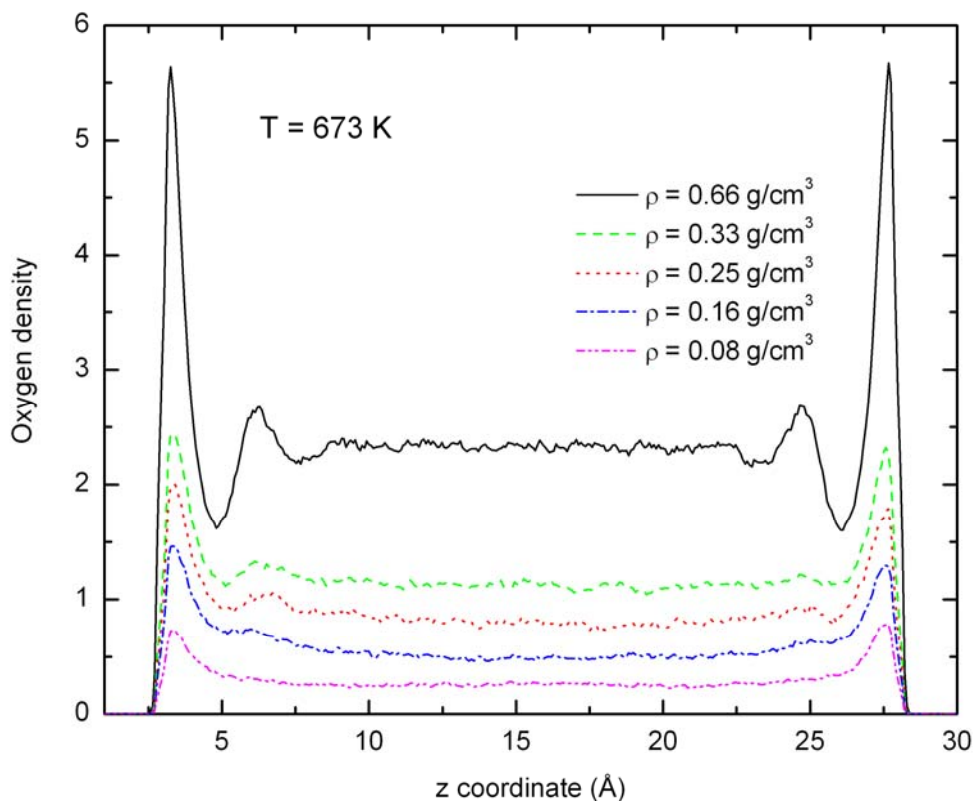


**Figure 2:** Oxygen density profiles of water molecules at  $T=673\text{K}$  and different densities

### Occupation and Residence Times

In Table 1 the percentages of water molecules located in the different regions are reported and they are compared with previous results at ambient [2] and high temperature [4] conditions. According to our findings, the occupation of the adsorbed layer is almost insensitive to the temperature. On the other hand, at  $T=673\text{K}$  we observe that this occupation systematically increases as the density diminishes. (Note that at  $T=298\text{K}$  and  $T=473\text{K}$  an intermediate layer located between the adsorbed and the central bulklike regions was observed [2,4]).

The residence time of a water molecule in a given region ( $\tau_{\text{res}}$ ) may be described as the average time spent by the molecule in such region before moving away. The  $\tau_{\text{res}}$  values listed in Table 1 were determined following the procedure described by Impey et al. [11]. At all temperatures,  $\tau_{\text{res}}$  in the adsorbed regions are significantly lower than in the bulk ones. As a general trend,  $\tau_{\text{res}}$  diminishes as temperature increases. At the supercritical temperature, we find that the residence time at the adsorbed region is much less dependent on the density than that corresponding to the bulk region. We think that this is due to the fact that  $\tau_{\text{res}}$  in the adsorbed layer is dominated by the strength of graphite-water interactions. On the contrary,  $\tau_{\text{res}}$  in the bulk region is mainly due to water-water interactions leading to a significant diminution of the residence time as  $\rho$  diminishes.

**Table 1:** Percentage of occupation of the different regions, residence times of the water molecules, mean number of hydrogen bonds per molecule and static dielectric constant.

T/K	$\rho/\text{gcm}^{-3}$	region	% occupation	$\tau_{\text{res}}/\text{ps}$	$n_{\text{HB}}$	$\epsilon$
673	0.660	adsorbed	21	5.4	1.18	8.4
		bulk	79	74.6	1.50	4.5
		total			1.40	4.6
673	0.330	adsorbed	22	3.7	0.81	4.4
		bulk	78	73.6	0.97	2.9
		total			0.92	3.0
673	0.250	adsorbed	24	3.6	0.66	3.2
		bulk	76	67.9	0.78	2.2
		total			0.74	2.4
673	0.160	adsorbed	26	3.7	0.53	2.5
		bulk	74	58.4	0.63	1.5
		total			0.61	1.8
673	0.080	adsorbed	27	4.0	0.23	1.2
		bulk	73	52.1	0.25	0.7
		total			0.25	0.8
298	1.000	adsorbed	23 <sup>a</sup>	54.0 <sup>a</sup>	3.20 <sup>a</sup>	172 <sup>b</sup>
		intermediate	17 <sup>a</sup>	14.0 <sup>a</sup>	3.50 <sup>a</sup>	30 <sup>b</sup>
		bulk	60 <sup>a</sup>	127.0 <sup>a</sup>	3.55 <sup>a</sup>	35 <sup>b</sup>
		total			3.48 <sup>a</sup>	85 <sup>b</sup>
473	0.863	adsorbed	20 <sup>c</sup>	16.0 <sup>c</sup>		34 <sup>c</sup>
		intermediate	19 <sup>c</sup>	7.5 <sup>c</sup>		19 <sup>c</sup>
		bulk	61 <sup>c</sup>	58.0 <sup>c</sup>		30 <sup>c</sup>
		total				27 <sup>c</sup>
633	0.526	adsorbed	20 <sup>c</sup>	5.2 <sup>c</sup>		8.3 <sup>c</sup>
		bulk	80 <sup>c</sup>	74.4 <sup>c</sup>		5.8 <sup>c</sup>
		total				5.8 <sup>c</sup>

<sup>a</sup> from Ref. [2], <sup>b</sup> from Ref. [3], <sup>c</sup> from Ref. [4]

## Hydrogen Bonding

As in previous studies of aqueous systems at supercritical conditions [12, 13], we adopted a geometric definition of the hydrogen bonds, i. e. we assumed that two water molecules were H-bonded if the next three geometrical conditions were fulfilled:

1. The distance  $R_{OO}$  between the oxygen atoms is smaller than  $R_{OO}^c$ ,
2. The distance  $R_{OH}$  between the "acceptor" oxygen and the hydrogen "donor" atoms is smaller than  $R_{OH}^c$ ,

3. The H--O...O angle  $\varphi$  is smaller  $\varphi^c$ .

The cut-off distances  $R_{OO}^c = 3.5 \text{ \AA}$  and  $R_{OH}^c = 2.4 \text{ \AA}$  were obtained from the first minima of the corresponding radial distribution functions  $g_{OO}(r)$  and  $g_{OH}(r)$ . The angular cut-off was chosen to be  $\varphi^c = 30^\circ$ .

As can be seen from Table 1, the mean number of hydrogen bonds per molecule ( $n_{HB}$ ) is slightly lower in the adsorbed layer than in the central bulklike region. The same tendency was found at ambient conditions [3]. On the other hand, at  $T=673\text{K}$ , the difference between  $n_{HB}$  for the two regions becomes less significant as density diminishes. It is worthy to remark that at the lowest density, i.e. for  $\rho = 0.08 \text{ g cm}^{-3}$ , the obtained value, namely  $n_{HB} = 0.25$ , should correspond to a practically monomeric structure.

### Static Dielectric Constant

The static dielectric constant  $\varepsilon$  can be computed as [14,15]

$$\varepsilon = 1 + \frac{4\pi \langle M^2 \rangle}{3Vk_B T} \quad (1)$$

where  $\langle M^2 \rangle$  is the averaged square dipole moment,  $V$  is the accessible volume, and  $k_B$  is the Boltzmann factor. The values of  $\varepsilon$  due to water molecules in adsorbed layers and bulk-like water are reported, together with the overall value, in Table 1.

At all temperatures, the value for  $\varepsilon$  is larger in the adsorbed layer than in the bulk region. This suggests the existence of a preferential orientation of the molecules close to the graphite walls. However, as temperature increases, the overall values of  $\varepsilon$  become closer to those from the bulk-like region, basically due to the increase of molecular disorder induced by the high thermal energies, which produce a loss of the orientational order of the molecular dipoles. Finally, at the supercritical temperature, we observe a drastic diminution of the static dielectric constant as density diminishes. Similar findings were obtained in a previous study of dielectric properties in bulk (unconfined) supercritical water [15].

### ACKNOWLEDGEMENTS

The authors gratefully acknowledge financial support from the “Generalitat de Catalunya” (Grant 2005SGR-00779), from the “Ministerio de Educación y Ciencia” of Spain (Grant FIS2006-12436-C02-01), and from European Union “FEDER” funds (UNPC-E015). J.S. is a recipient of a FPI Spanish fellowship.

### REFERENCES

- [1] WAS, G. S., AMPORNAT, P., GUPTA, G., TEYSSEYRE, S. WEST, E. A., ALLEN, T. R., SRIDHARAN, K., TAN, L., CHEN, Y. REN, X., PISTER, C., *J. Nucl. Mater.*, vol. 371, **2007**, p. 176

- [2] MARTÍ, J., NAGY, G., GORDILLO, M. C., GUÀRDIA, E., J. Chem. Phys., vol. 124, **2006**, p. 09473
- [3] MARTÍ, J., NAGY, G., GUÀRDIA, E., GORDILLO, M. C., J. Phys. Chem. B, vol. 110, **2006**, p. 23987
- [4] NAGY, G., GORDILLO, M. C., GUÀRDIA, E., MARTÍ, J., J. Phys. Chem. B., vol. 111, **2007**, p. 12524
- [5] SALA, J. GUÀRDIA, E., MARTÍ, J., to be submitted.
- [6] MARTÍ, J., PADRÓ, J. A., GUÀRDIA, E., J. Mol. Liq. vol. 62, **1994**, p. 17
- [7] LIEW, C. C., INOMATA H., ARAI, K., Fluid Phase Equilib., vol. 144, **1998**, p. 287
- [8] GORDILLO, M. C., MARTÍ, J., Chem. Phys. Lett., vol. 329, **2000**, p.341
- [9] BERENDSEN, H. J. C., POSTMA, J. P.M, VAN GUNSTEREN, W. F., DINOLA, A., HAAK, J. R. , J. Phys. Chem., vol. 81, **1984**, p. 3684
- [10] SPOHR, E., J. Chem. Phys., vol. 106, **1997**, p. 388
- [11] IMPEY, R. M., MADDEN, P. A., MCDONALD, I. R., J. Phys. Chem. vol. 87, **1983**, 5071.
- [12] MARTÍ, J., J. Chem. Phys., vol. 110, **1999**, p. 6876
- [13] GUÀRDIA, E., LARIA, D., MARTÍ, J., J. Phys. Chem. B, vol. 110, **2006**, p. 6332
- [14] DE LEEUW, S. W., PERRAM, J., SMITH, E. R., Proc. R. Soc. London Ser. A, vol. 388, **1983**, p. 177
- [15] GUÀRDIA, E., MARTÍ, J., Phys. Rev. E, vol. 69, **2004**, p.011502